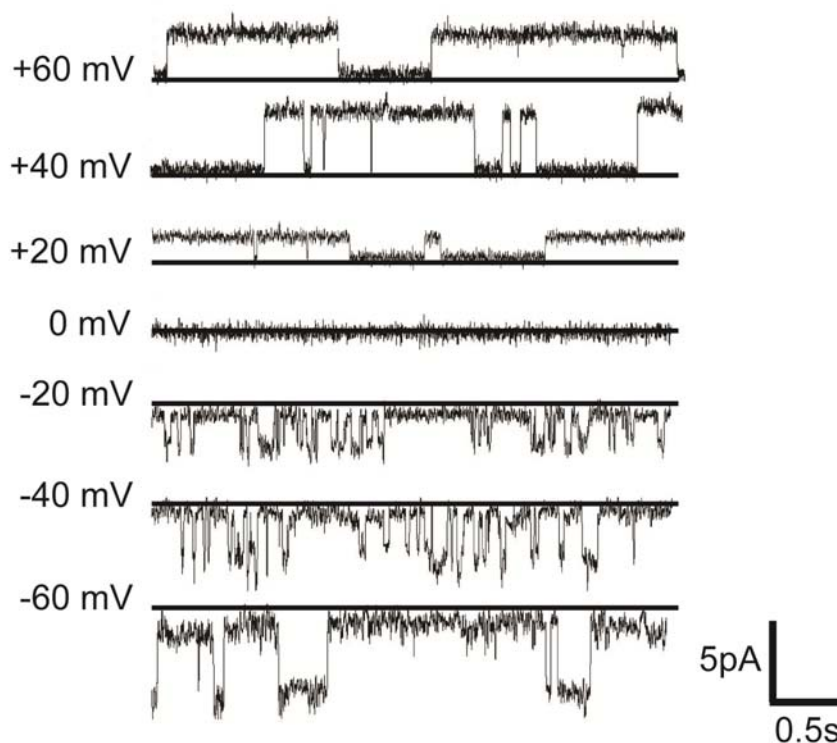
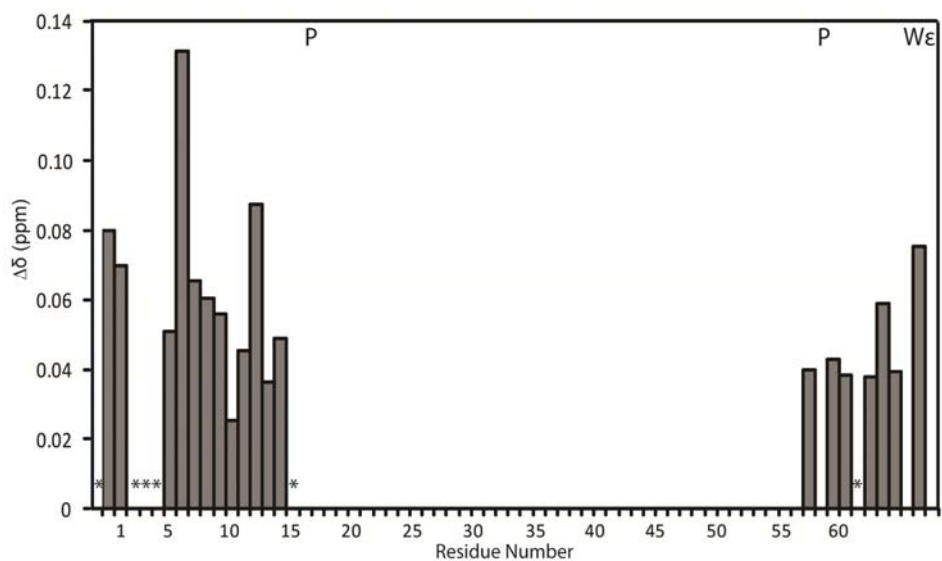


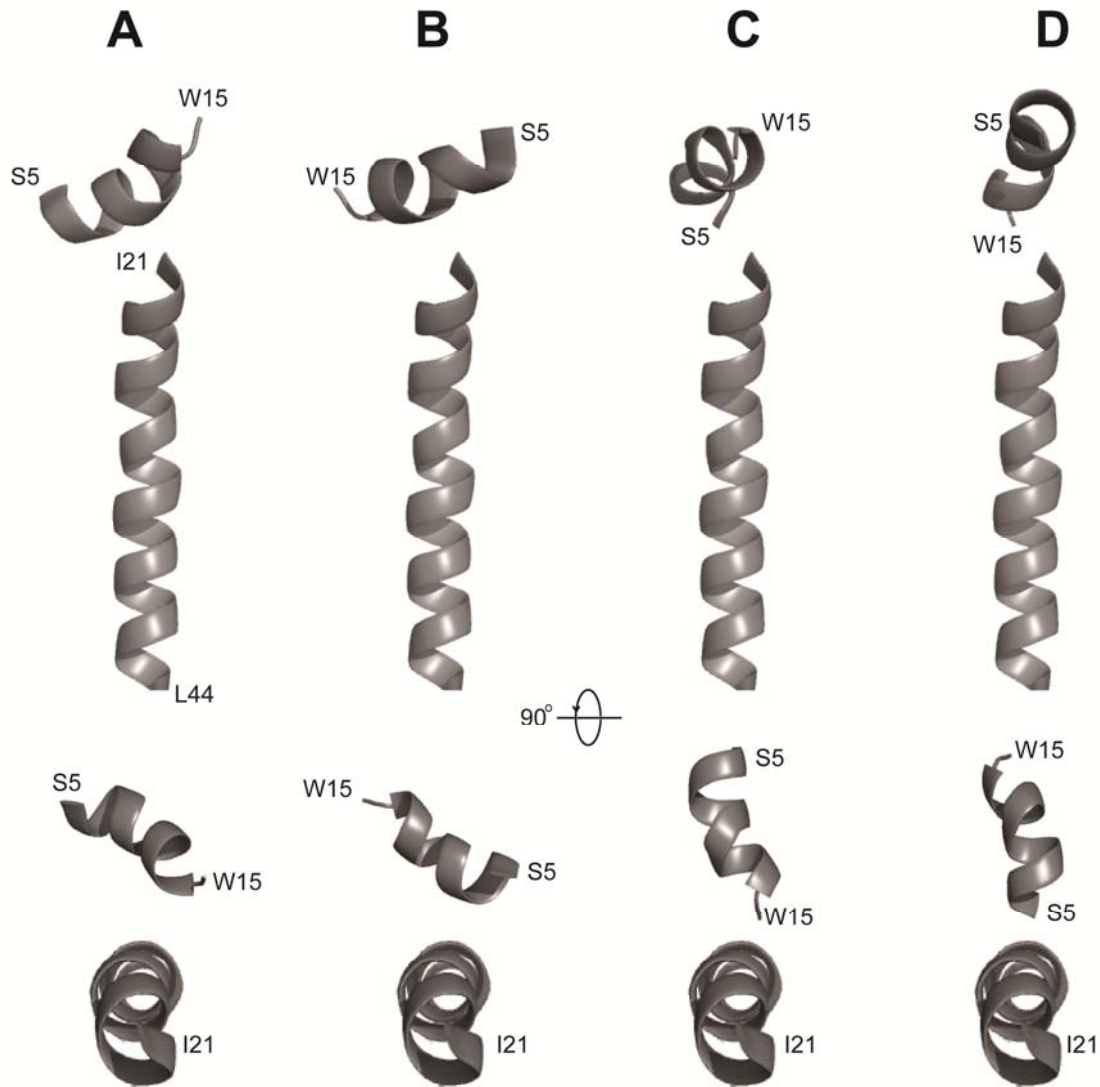
Supplementary Information



Supplementary Figure S1. Channel activity of purified full length SH protein conductance in black lipid membranes. Current traces recorded at different voltages. The bilayers used were DPhPC. For the preparation of SH proteoliposomes, SH protein was reconstituted into liposomes formed by DPhPC and cholesterol (10:1 molar ratio, Avanti Polar Lipids), at a 1:100 protein/lipid (mol/mol) ratio. Giant unilamellar vesicles were prepared by electroformation on a Nanion Vesicle Prep Pro setup (Nanion Technologies GmbH, Munich, Germany). Electrophysiological recordings were carried out with a Port-a-Patch automated patch clamp system (Nanion Technologies GmbH, Munich, Germany). First, a planar bilayer was obtained by applying 5 μ l of GUV solution onto the borosilicate glass chips, \sim 1 μ m aperture, in presence of a slightly negative pressure (-20 mbar). The formation of the planar lipid bilayer on the aperture provided a seal resistance of >10 G Ω . Then, proteoliposomes containing SH protein were pipetted onto the planar lipid bilayer. Currents were amplified with Axon Patch 200B amplifier (Axon instruments, USA). The data were acquired by using Axon Digidata 1322A and analyzed with Clampfit (Axon instruments, USA). The experiment was performed in a symmetric solution of 150 mM NaCl, 5 mM HEPES at pH 5.1. Attempts to use a higher pH resulted in a broken membrane.



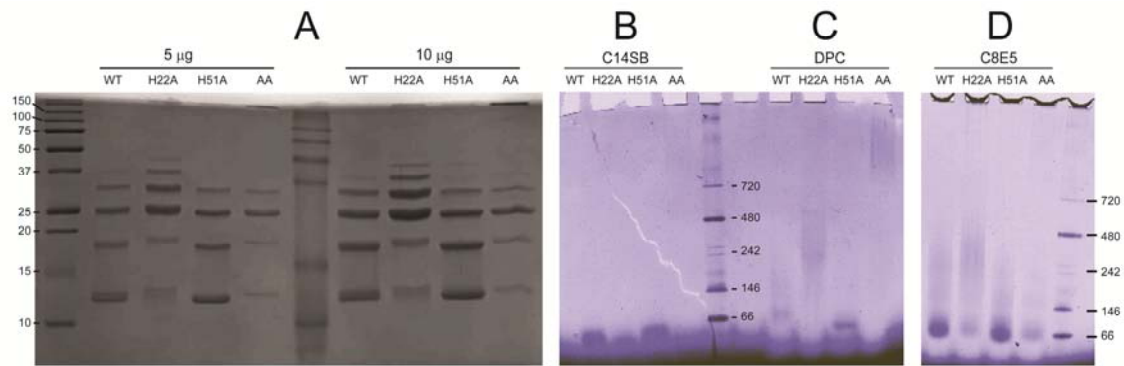
Supplementary Figure S2. Chemical shift difference ($\Delta\delta$) for peaks showing doubling in the Trosy-HSQC spectra. Shift difference between doubled peaks (pairs) at each residue position. Conformational exchange occurs mainly in the N-terminal helix and at the flexible tail of the C terminus. P represents proline residues, W ϵ represents the sidechain of W15, * represents peaks where conformational doubling cannot be ascertained.



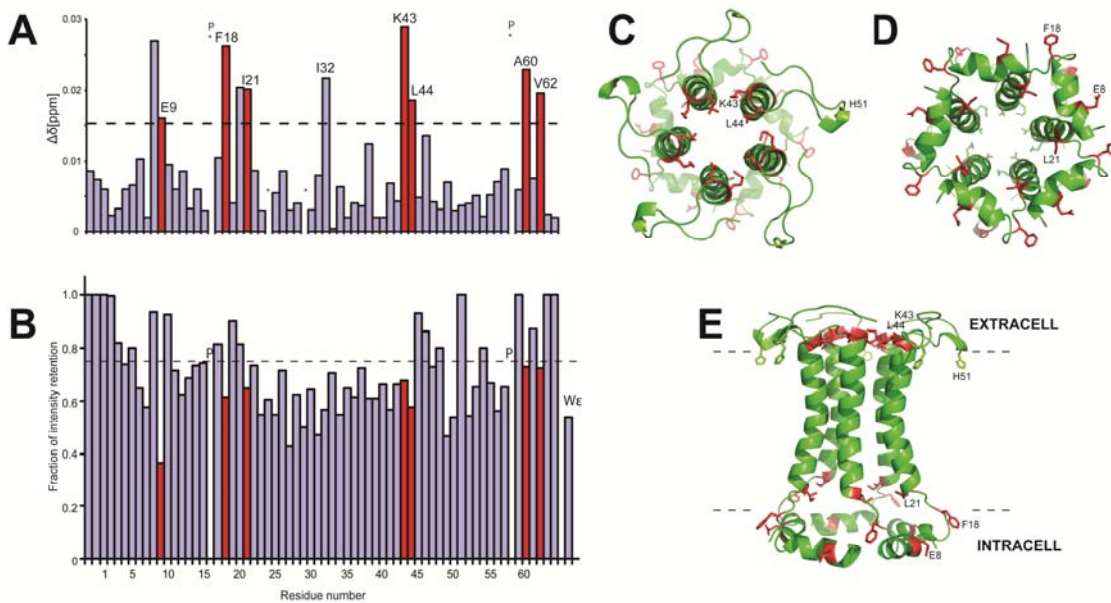
Supplementary Figure S3. RDC-derived models for the SH monomer. Side views (top) and top views (bottom) of four models (A-D) for the N-terminal helix (S5-W15) and TM helix (I21-L44) of SH protein. The TM is in the same orientation in all four models, and the N-terminal helix is perpendicular to the TM helix. The C terminal β -turn has been removed for clarity. Models were derived from the mean structure from CYANA, where flexible residues at the termini (M1-T4) and (R59-T64) were excluded to avoid fraying effects. Figures were rendered in Pymol [1]. Of the 4 four possibilities, model C shows the best fit to the paramagnetic mapping and titration data.

Supplementary Table S1. Enforced restraints for HADDOCK. 15 intermonomeric pairings were implemented as enforced restraints for HADDOCK. Full flexibility of the NOEs was defined, using van der Waals (VDW) as lower limits, and 4.5 Å as upper limit.

Interacting pair		
From	To	
S5 HN	W15 HB3	N-terminal domain NOEs
S5 HN	K14 HD	
I6 HD1	P16 HD2	
I6 HD1	P16 HD3	
I6 HD1	P16 HA	
T7 HB	P16 HG	
T7 HB	P16 HD2	
I28 HB	S29 HB	TM domain NOEs
I28 HD1	S29 HB	
L41 HG	I40 HA	
S35 HA	I33 HB	
S35 HB2	I33 HA	
S35 HB2	I33 HG2	
S35 HB3	I33 HG1	
S35 HB3	I33 HG2	



Supplementary figure S4. Electrophoretic mobility of WT and His to Ala mutations. (A) SDS gel; (B-D) BN-PAGE gels where the sample was presolubilized in the detergents indicated above.



Supplementary Figure S5. Chemical shift and intensity perturbation of SH protein residues after addition of 50 μM Cu^{2+} . (A) Chemical shift perturbation ($\Delta\delta$); (B) Fraction of retained intensity after normalization relative to initial intensity before adding Cu^{2+} . We represents the sidechain of W15. In both graphs, residues in red indicate a large perturbation in both chemical shift and intensity. Cut-offs are arbitrary values; (C) Perturbed residues (in red) at the C-terminal mouth of the pore; (D) Same for the N terminal mouth of the pore; (E) Side view. H51 is only shown as a reference.

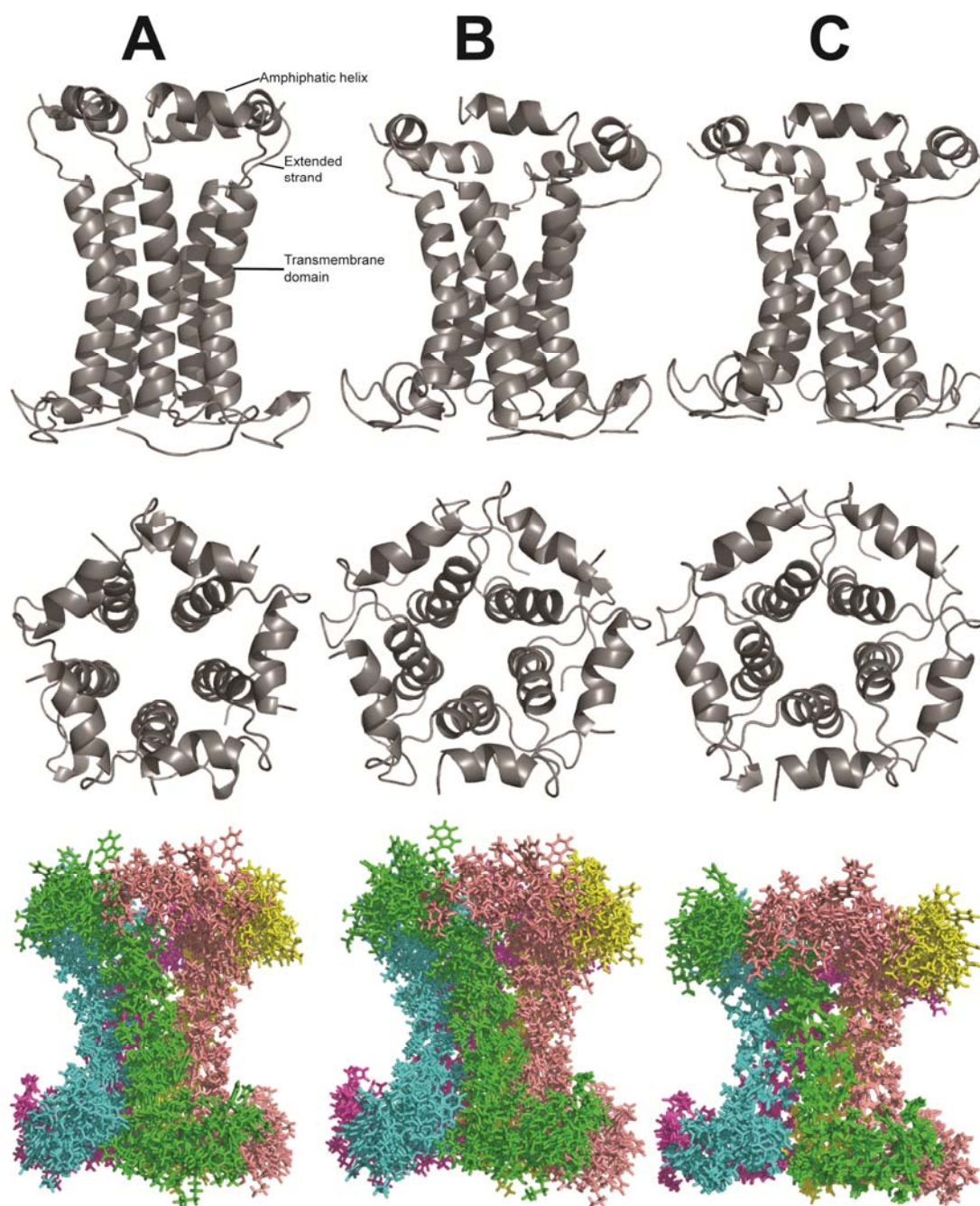
```

YP_138516 PIV5      MLP DPEDPESKKATRRAAGNLIIC FLFIFFLFVTFIVP TLRHLLS
BAA13028 mump S    MPAIQPPLYL TFLLLILLYMII TLYVWIIL TITYKTAVRHAALYQG SFFRWSFDHSL

VSH_HRSVA         M ENT SITIEFSSKFWPYFTLIHMIIISLLIIISIMIAIL NKLCEYNVFNKTFELPRA RVNT
ABV24742          M ENT SITIEFSSKFWPYFSLIHMIIISLLIIISIMIAIL NKLCEYNVFNKTFELPRA RVNT
ABV24776          M ENT SITIEFSSKFWPYFTLIHMIIISLLIIISIMIAIL NKLCEYNVFNKTFELPRA RVNT
AA028132          MGN TSITIEFTSKFWPYFTLIHMILTLISLLIIITIMIAIL NKLSEHKTFCKNTLEGGQMYQINT
HRSV              MGN TSITIEFTSKFWPYFTLIHMILTLISLLIIITIMIAIL NKLSEHKPFCKNTLEGGQMYQINT
ABV24839          MVN TSITIEFTSKFWPYFTLIHMILTLISLLIIITIMIAIL NKLSEHKAFCKNTLEGGQMYQINT
HRSV3             MGN TSITIEFTSKFWPYFTLIHMILTLISLLIIITIMIAIL NKLSEHKRFCKNTLEGGQMYQINT
ABV24836          MGN TSFTIEFTSKFWPYFTLIHMILTLISLLIIITIMIAIL NKLSEHKIFCKNTLEGGQMYQINT
AA028118(transl cRNA) MGN TSITIEFTSKFWPYFTLIHMILTLISLLIIITIMIAIL NKLSEHKTFCKNTLEGGQMYQINT
ABV24841          MGN TSITIEFTSKFWPYFTLIHMILTLISLLIIITIMIAIL NKLSEHKTFCKNTLEGGQMYQINT
AAR14264          MGN TSITIEFTSKFWPYFTLIHMILTLISLLIIITIMIAIL NKLSEHKTFCKNTLEGGQMYQINT
VSH_HRSV8         MGN TSITIEFTSKFWPYFTLIHMILTPISLLIIITIMIAIL NKLSEHKTFCKNTLEGGQMYQINT
AAB82434          MGN TSITIEFTSKFWPYFTLIHMILTLISLLIIITIMIAIL NKLSEHKTFCKNTLEGGQMYQINT
VSH_BRSVA (bovin e) MNN TSTMI EFTGKFWYFTLVFMMLIIGFFFVITSLVAAIL NKLCDLNDHHTNSLDIRTLRNDTQSITRAHV
AAL49408          MNN TSTMI EFTGKFWYFTLVFMMLIIGFFFVITSLVAAIL NKLCDLNDHHTNSLDIRTLRNDTQSITRAHV
AA032982          MNN TST IIEFTDKFWYFSLVFMMLIIGFFVIVTSLVAAIL NKLCVLSNHHHTNSLDIRTLRNDTQSITRAHEGSINQSSN
AA032981          MNN TST IIEFTDKFWYFSLVFMMLIIGFFVIVTSLVAAIL NKLCVLSNHHHTNSLDIRTLRNDTQSITRAHEGSINQSSN
VSH_BRSV3         M NSTST IIEFTGKFWYFTLVFMMLTIGFFFIVTSLVAAIL NKLCDLNDHHTNSLDIRTKLRSDTQLITRAHEESINQSSN
AA032980          MNN TST IIEFTGKFWYFTLVFMMLTIGFFF IITSLAAAIL NKLCDLNDHHTNSLDIRTLRNDTQLITRAHEGQINQSSN
* . * * : : * * * * * * : : : : * * * * * . . . : : :
VSH_HRSVA         M ENT SITIEFSSKFWPYFTLIHMIIISLLIIISIMIAIL NKLCEYNVFNKTFELPRA RVNT

```

Supplementary Figure S6. Multiple alignment of SH protein in human and bovine RSV. For comparison, on top of the alignment, the sequences of PIV5 and mumps virus SH protein are also indicated. His residues are highlighted in yellow. The sequence used in the present paper is VSH_HRSVA, which is also placed at the bottom of the alignment, below the symbols that indicate degree of conservation.



Supplementary Figure S7. Overall structure of the SH pentamer. Structures of the top 3 scoring clusters from HADDOCK depicting the side view (top), the top view (middle) and overlay of 4 best structures of cluster (bottom); (A) Best structure with lowest HADDOCK score; (B) Best structure with largest cluster size; (C) Best structure with lowest RMSD to lowest energy structure. The structures vary in the position of the N-terminal helices, with A being the furthest away from the TM domain, where helices are more tightly packed to each other. The N-terminal helices in B and C are positioned closer to the TM domain, and therefore are splayed or extended outwards.

1. DeLano WL The PyMOL Molecular Graphics System. DeLano Scientific LLC, San Carlos, CA, USA.